ATRP-Inspired Room Temperature (sp^3)C–N Coupling

Alfred. K.K. Fung, Li-Juan Yu, Michael S. Sherburn* and Michelle L. Coote*

ARC Centre of Excellence for Electromaterials Science, Research School of Chemistry, Australian National University, Canberra, Australian Capital Territory 2601, Australia

*Email: Michael.Sherburn@anu.edu.au; michelle.coote@anu.edu.au

ABSTRACT: A simple non-photochemical procedure is reported for Cu(I)-catalyzed C–N coupling of aliphatic halides with amines and amides. The process is loosely based on the Goldberg reaction but takes place readily at room temperature. It uses Cu(I)Br, a commonly-used and inexpensive atom transfer radical polymerization (ATRP) precatalyst, along with the cheap ligand *N,N,N′,N″,N″*-pentamethyldiethylenetriamine (PMDETA), to activate the R–X bond of the substrate via inner-sphere electron transfer. The procedure brings about productive C–N bond formation between a range of alkyl halide substrates with heterocyclic aromatic amines and amides. The mechanism of the coupling step, which was elucidated through application of computational methods, proceeds via a unique Cu(I)→ Cu(II)→Cu(III)→Cu(I) catalytic cycle, involving (a) inner-sphere electron transfer from Cu(I) to the alkyl halide to generate the alkyl radical; (b) successive coordination of the N-nucleophile and the radical to Cu(II); and finally reductive elimination. In the absence of a nucleophile, debrominative homocoupling of the alkyl halide occurs. Control experiments rule out S_N-type mechanisms for C–N bond formation.

INTRODUCTION

There exists a plethora of cross-coupling methods for the formation of C–N bonds.[1] Buchwald-Hartwig amination revolutionized the formation of (sp^2)C–N bonds by the introduction of a Pd(0)/Pd(II) catalytic cycle for cross-coupling. The process greatly extended the scope of Cu(I)-catalyzed Ullmann-type (sp^2)C–N bond formation, through the introduction of significantly milder reaction conditions and complementary electrophile reactivity. Nonetheless, as demonstrated by recent photoredox-based approaches, [2, 3] there is a pressing need for better methods for (sp^3)C–N bond formation, and for the replacement of rare metals with earth-abundant ones.[4]

The simplest way to make an (sp^3)C–N bond is by direct (i.e. uncatalyzed) nucleophilic substitution. The main problem with a classical S_N2 approach (Scheme 1) is the tendency for competing amine polyalkylation and alkyl halide elimination. Important advances have been recently described by the Nishikata[5] and Fu[6] laboratories through the invention of Cu(I)/Cu(III)-based catalytic cycles.

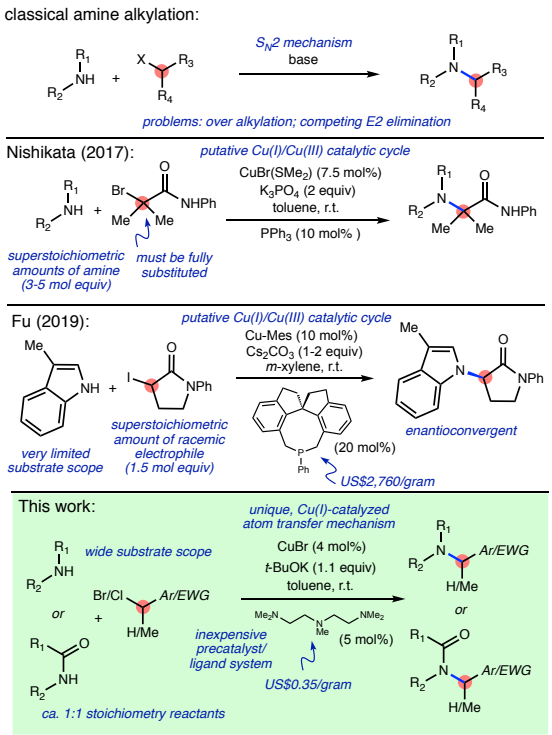

Scheme 1. The classical S_N approach, state-of-the-art methods[5, 6] and the current work on non-photochemical Cu(I)-catalyzed (sp^3)C–N cross-coupling.

These approaches, which bring about C–N bond formation under mild and photochemistry-free conditions, permit the generation of products that are not feasible through direct S_N2 based processes.

Herein, we describe a new Cu(I)-catalyzed method for (sp^3)C–N bond formation that is mechanistically distinct from both Ullmann-type processes and the Nishikata/Fu Cu(I)–Cu(III) catalytic cycle. Our method is effective over a broader range of substrates and, importantly, is effective with 1:1 precursor stoichiometry. Akin to photoredox catalysis methods, our approach involves carbon-centered radical intermediates. Our method uses ambient reaction conditions and inexpensive and readily available catalysts and reagents (Scheme 1). Our method is also photochemistry-free, hence applicable to light-sensitive substrates and products.

Our approach takes advantage of the highly active catalysts developed for carbon-centered radical generation from alkyl halides in atom transfer radical polymerization (ATRP).[7, 8] In ATRP, a Cu(I) catalyst reversibly generates a low concentration of carbon-centered radicals from "dormant" alkyl halides in order to control radical polymerization (Scheme 2). Originally based on atom transfer radical addition (ATRA) methodologies,[9] successive generations of Cu(I) catalysts have led to an improvement in activity of more than 7 orders of magnitude simply by varying the ligand (Figure 1).[10-12] As a result, currently available catalysts can trigger the reversible cleavage of relatively strong (sp^3)C–X bonds at room temperature at low catalytic loading.[13] Until now, these catalysts have been used to generate radicals exclusively for ATRP and ATRA processes. Herein we demonstrate for the first time that their enhanced reactivity can be harnessed for (sp^3)C–N coupling processes to achieve outcomes akin to those from photoredox-based methods, but without irradiation and under mild conditions.

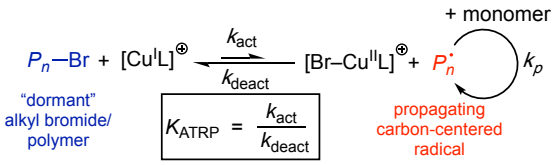

Scheme 2. Generalized mechanism of ATRP.

As proof of concept for our process, we use copper(I) bromide and *N,N,N′,N″,N″*-pentamethyldiethylenetriamine (PMDETA) as cheap and readily available precatalyst and ligand. Whilst PMDETA is not the most active ligand available,[10] it is attractive as it is low in cost and easy to obtain. As will be shown, the *in situ*-generated [(PMDETA)Cu(I)Br] catalyst is sufficiently reactive to outcompete uncatalyzed processes such as S_N2 processes and base-mediated eliminations, even in the presence of *t*-BuOK.

RESULTS AND DISCUSSION

Reaction Development. The conversion of benzotriazole **1** and benzyl bromide **2** into 1-benzyl benzotriazole **3** proceeds at ambient temperature in toluene using low loadings of the precatalyst Cu(I)Br and the ligand PMDETA in the presence of a stoichiometric amount of *t*-BuOK (Table 1, entry 1). This precatalyst/ligand combination was chosen since it has been previously optimized for ATRP processes.[14] The

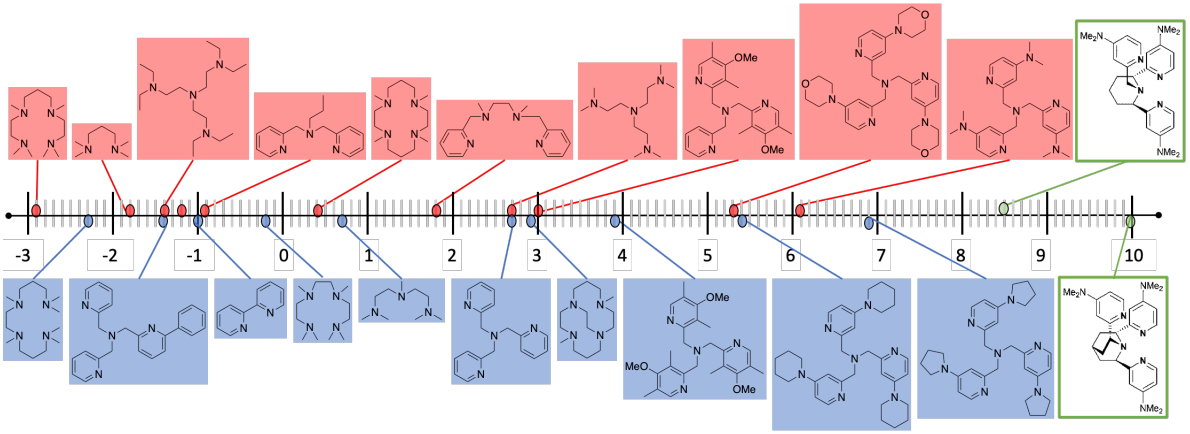

Figure 1. Selected experimental activation rate constants log(k_{act} /(M^{-1} s^{-1})) for ATRP involving various N-based ligands with the initiator $CH_3CH_2(COOCH_3)Br$ in the presence of Cu^{I}Br in MeCN at 22 °C. Computational values are shown for the ligands in green boxes. Figure reproduced with permission from Ref.[15].

conversion of **1** + **2** → **3** has been previously carried out under S_N2 conditions, using a large excess of concentrated aqueous NaOH in MeCN.[16] This published reaction presumably involves the *in situ* conversion of the acidic (pK_a = 8.2)[17] benzotriazole (**1**) into its more nucleophilic, conjugate base. A repeat of our entry 1 reaction but omitting the Cu(I)Br precatalyst and PMDETA (entry 2) gave no detectable conversion of **1** + **2** → **3**, thereby dismissing the uncatalyzed S_N2 mechanism for entry 1. It seems reasonable to assume that the nonpolar toluene solvent inhibits the *t*-BuOK-induced formation and S_N2 reaction of the conjugate base of **1**.

Table 1. Reaction Development. Isolated yields of C–N cross-coupling product **3** from the reaction of benzotriazole **1** and benzyl bromide **2**, as a function of reactant, precatalyst (Cu(I)Br) and ligand (PMDETA) molar ratios, and solvent.

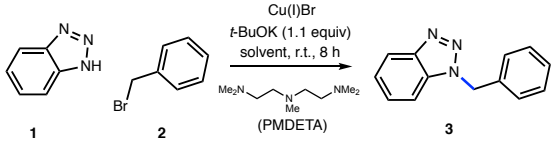

Entry	Molar Ratios Used				Solvent	Yield 3 (%)
	Cu(I)Br	PMDETA	1	2		
1	0.05	0.1	1.0	1.0	PhMe	86
2	0	0	1.0	1.0	PhMe	0
3	0.01	0.02	1.0	1.0	PhMe	63
4	0.20	0.29	1.0	1.0	PhMe	89
5	0.50	0.58	1.0	1.0	PhMe	33
6	0.20	0.29	1.6	1.0	PhMe	93
7	0.20	0.29	1.0	1.8	PhMe	89
8	0.20	0.29	1.0	1.0	CH_2Cl_2	87
9	0	0	1.0	1.0	CH_2Cl_2	0
10	0.20	0.29	1.0	1.0	Et_2O	89
11	0	0	1.0	1.0	Et_2O	0
12	0.20	0.29	1.0	1.0	DMSO	88
13	0	0	1.0	1.0	DMSO	61
14	0.20	0.29	1.0	1.0	MeCN	92
15	0	0	1.0	1.0	MeCN	71

Precatalyst/ligand loadings from low to moderate levels (entries 3 and 4) do not have an adverse effect upon the process, although very high loadings (entry 5) result in lower yields of C–N coupled product, accompanied by the formation of significant amounts of 1,2-diphenylethane.

The reaction is also tolerant of changes in precursor stoichiometry, with yields high, irrespective of whether **1** or **2** is the limiting reactant (entries 6 and 7). These observations identify a significant advantage over recently-published Cu(I)-catalyzed C–N couplings (Scheme 1), which need superstoichiometric amounts of either the amine[5] or alkyl halide[6] reactant.

Since the ATRP activity of the [PMDETA]Cu(I)Br] complex increases with solvent polarity,[18] we recognized a switch to more polar solvent systems may be advantageous. Our C–N coupling reaction is effective over a range of solvents (entries 8-15). There is no competing S_N2 process in dichloromethane and diethyl ether (entries 8-11) but the uncatalyzed process also occurs in the most polar solvents DMSO and MeCN (entries 12 -15).

Experimental Mechanistic Studies. In order to further probe the requirements for successful C–N coupling, the reaction between carbazole **4** and 1-bromoethylbenzene **5** was examined under a range of conditions (Table 2). Interestingly, the conversion **4** + **5** → **6** has not previously been described, although the molecule has been recently prepared by Fe(III) and Cu(I)-catalyzed hydroamination of styrene with carbazole[19, 20] and base-mediated coupling of acetophenone tosylhydrazone with carbazole.[21]

The reaction proceeds smoothly under standard conditions (Table 2, entry 1) but, once again, no product is observed in the absence of Cu(I)Br (entry 2). Consistent with previous observations of its significant rate enhancement in ATRP chemistry, the PMDETA ligand is also necessary for C–N coupling (entry 3).

The absence of *t*-BuOK (entry 4) results in a low but still notable yield of product **6**, which signals the possibility of the tertiary amine groups of the PMDETA ligand serving as base. In ATRP, this causes a decrease in binding of PMDETA to the metal center, thereby deactivating the catalytically active species.[22] The use of either Et_3N or Cs_2CO_3 in place of *t*-BuOK (entries 5 and 7) gave similar yields of product **6**. No product is observed in the absence of Cu(I)Br with each of these alternative bases (entries 6 and 8). We generally favor the use of *t*-BuOK as base since it gives optimal yields across a broader range of substrates.

As entry 9 shows, the reaction does not require photo-activation, perhaps unsurprisingly given the proposed structure of the catalytic species. The reaction has inherited some level of oxygen sensitivity from ATRP,[23] resulting in the need to

thoroughly degas solvents before execution (entry 10).

Table 2. Control Experiments. Yields of C–N cross-coupling product **6** for reactions of carbazole **4** and 1-bromoethyl benzene **5** with variations from the standard conditions.[a]

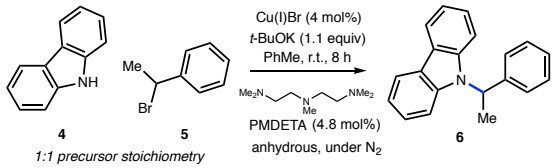

Entry	Conditions	Yield 6 (%)
1	As specified in the equation	81
2	No Cu(I)Br	0
3	No PMDETA	0
4	No *t*-BuOK	18
5	Et_3N in place of *t*-BuOK	75
6	Et_3N in place of *t*-BuOK, no Cu(I)Br	0
7	Cs_2CO_3 in place of *t*-BuOK	78
8	Cs_2CO_3 in place of *t*-BuOK, no Cu(I)Br	0
9	No ambient light	65
10	Open flask, vigorous stirring	0
11	Cu(I)Br (50 mol%), PMDETA (58 mol%)	27

Entry 11 shows, once again (cf. Table 1, entry 5), that high precatalyst/ligand loadings lead to homocoupling as a competing process. With bromide **5**, 2,3-diphenylbutane was isolated. These unoptimized reactions show the potential of ATRP catalysts in (sp^3)C–(sp^3)C bond formation, consistent with earlier experiments on polystyryl alkyl halides.[24] Potentially, high precatalyst/ligand loadings result in increased amounts of benzylic free radicals, which would undergo direct radical-radical coupling to form these bibenzyl compounds.

Computational Mechanistic Studies. To ascertain the most likely mechanism for our C–N cross-coupling process, density functional theory calculations were performed using, as a case study, the reaction between carbazole **4** (as the amine or its conjugate base) and 1-bromoethyl benzene **5**. Full details of the theoretical study are provided in the Supporting Information. The mechanism of carbon-halogen bond activation for this catalyst and substrate has been studied previously within the context of ATRP.[25, 26] Under ATRP reaction conditions, complexation of the tridentate, electron-rich PMDETA ligand to Cu(I)Br to form neutral complex **7**, results in dissociation of the bromide ion to form the catalytically active cationic species **8** (Scheme 3). Activation of the carbon-bromine bond then proceeds via a reversible inner-sphere electron transfer (ISET) with the alkyl halide **9**, which results a concerted reductive cleavage of the C–Br bond to form carbon-centered radical R• **11** and Cu(II) complex **10**.

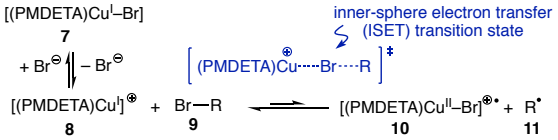

Scheme 3. The mechanism of carbon-halogen bond activation in ATRP.

In the present work, our conditions differ from ATRP in two crucial aspects: (a) deprotonated nucleophile is present; (b) a non-polar solvent, toluene, is used in place of acetonitrile. Under, these conditions dissociation of the [(PMDETA)Cu^{I}Br] catalyst **7** is strongly thermodynamically disfavored, although reversible ligand exchange with the deprotonated amine nucleophile to form [(PMDETA)Cu^{I}(NR'$_2$)] **12** is possible (Scheme S1, Supporting Information). Both of these species are capable of undergoing ISET reactions with the substrate to form a neutral Cu^{II} species, [(PMDETA)Cu^{II}Br(NR'$_2$)]• **15** or [(PMDETA)Cu^{II}Br$_2$]• **11** respectively (Scheme S2, Supporting Information). Our calculated equilibrium constant for the exchange reaction favors [(PMDETA)Cu^{I}(NR'$_2$)] **12** over [(PMDETA)Cu^{I}Br] **7** by a factor of 1078, but the latter species undergoes the subsequent ISET process with a rate coefficient that is 7788 times higher, and thus is the dominant pathway overall by a factor of 7. However, carbazole **4** is quite sterically hindered, and thus one would expect the ISET reactions of [(PMDETA)Cu^{I}(NR'$_2$)] **12** to become more competitive for less hindered nucleophiles. In any case, any [(PMDETA)Cu^{II}Br$_2$]• **11** formed, readily undergoes ligand exchange with $^{\ominus}$NR'$_2$ to form [(PMDETA)Cu^{II}Br(NR'$_2$)]• **15**.

As in standard ATRP, the corresponding outer-sphere (OSET) processes have Marcus theory barriers more than 100 kJ mol^{-1} higher than the ISET pathways and can thus be discounted (Scheme S2, Supporting Information). Due to

steric crowding, viable oxidative addition transition states could not be located for these tetradentate Cu^{I} species, and we note that these pathways have been likewise ruled out for related Ullman-type cross-coupling by Houk, Buchwald and coworkers.[27]

Once $[(PMDETA)Cu^{II}Br(NR'_2)]^{\bullet}$ **15** forms, it then undergoes barrierless radical coupling with $R^{\bullet}$ **11** to form a triplet species that is effectively a weak π-complex of $R^{\bullet}$ **11** with $[(PMDETA)Cu^{II}Br(NR'_2)]^{\bullet}$ (see Figure S2.3, Supporting Information). This undergoes an intersystem crossing through a modest barrier of 60 kJ mol^{-1} to form an open-shell singlet $[(PMDETA)Cu^{III}BrR(NR'_2)]$ **16**, in which the R-group is formally coordinated. This is then kinetically trapped by an almost barrierless reductive elimination to form the cross-coupled product, $R–NR'_2$ **17**, and to regenerate the catalyst, $[(PMDETA)Cu^{I}Br]$ **7**. The overall mechanism thus involves a fascinating Cu(II)→Cu(III)→Cu(I) catalytic cycle (Scheme 4).

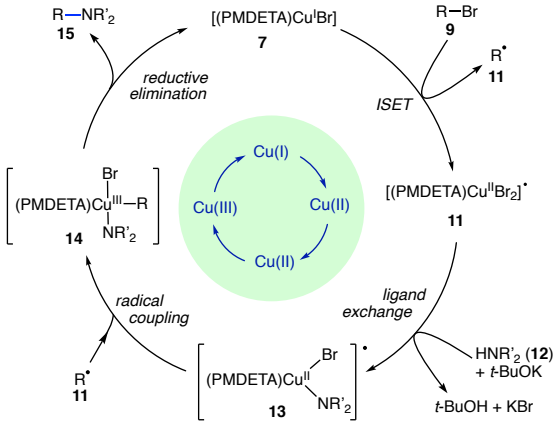

Scheme 4. The most favored cross-coupling pathway. The corresponding Gibbs free energies are provided in the SI. An alternative process in which Br/NR_2' ligand exchange occurs prior to the ISET reaction, rather than after, is likely to contribute, particularly for less hindered nucleophiles and is shown in Figure S2.5 of the Supporting Information.

Scope. To explore the scope of the C–N coupling process, we first investigated variations in the nitrogen-based component, while restricting the alkyl halide to primary and secondary benzyl halides (Table 3). Control experiments revealed that piperidine, *t*-butyl amine and aniline reacted through uncatalyzed S_N2 processes, hence only less reactive N-based coupling partners were deployed. Thus, in addition to benzotriazole **1** (Table 1) and carbazole **4** (Table 2), 7-azaindole **18**, 1,2,4-triazole **19**, 3,5-dimethylpyrazole **20**, 2-methylimidazole **21**, benzamide **22** and 2-pyrrolidone **23** underwent benzylation and 1-methylbenzylation under mild, Cu(I)Br/PMDETA-catalyzed conditions with reactant molar ratios close to 1:1. Control experiments showed that no reaction occurred in the absence of precatalyst and ligand.

Table 3. $[(PMDETA)Cu^{I}Br]$-catalyzed benzylation and 1-methylbenzylation of heterocyclic amines and amides.

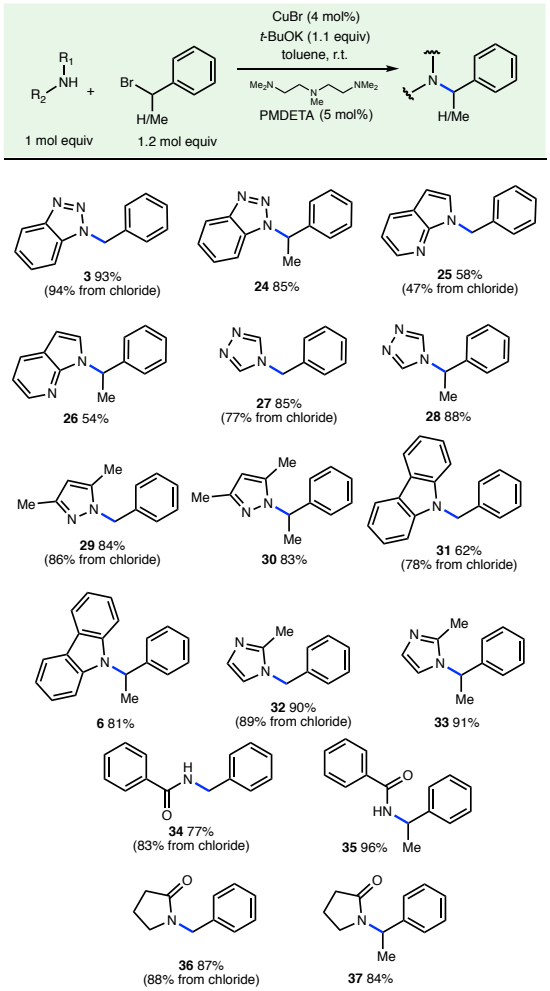

As shown in Table 3, for a given amine, benzyl chloride **38** and 1-chloroethylbenzene **39** furnished similar yields of C–N coupled products to the corresponding bromide. As has been demonstrated in ATRP studies, the chlorophilicity of the Cu(I) catalyst compensates to a large extent for the stronger R–Cl versus R–Br bond, resulting in similar reactivity and in this study, similar yields.[26] S_N2 processes are sensitive to substitution at the electrophilic carbon. The results depicted in Table 3 reveal a contrast to this

reactivity: for a particular amine/amide, primary and secondary benzyl halides react with a similar ease to furnish benzylated products in similar yields.

To unequivocally demonstrate that these C–N bond formations are the result of Cu(I)-catalyzed processes, the progress of reactions performed in toluene-d_8 were followed by ^{1}H NMR spectroscopy. As can be seen by inspection of Figure 2, when 2-pyrrolidone **23**, benzyl bromide **2**, and a stoichiometric quantity PMDETA (to serve as both soluble base and ligand) are mixed at ambient temperature in toluene-d_8, no detectable reaction occurs over a period of 24 hours. Upon addition of Cu(I)Br to this sample, smooth conversion to *N*-benzylpyrrolidone **36** is witnessed over an 8 hour period.

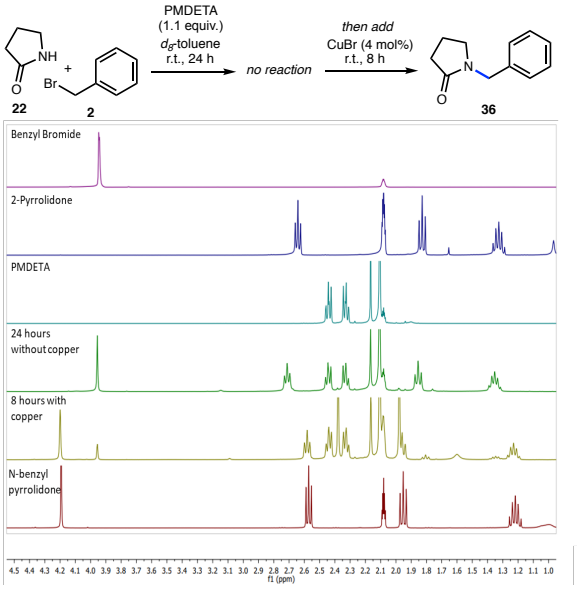

Figure 2. 400 MHz ^{1}H NMR stacked plots of the reaction between 2-pyrrolidone **23**, benzyl bromide **2**, PMDETA, and Cu(I)Br at ambient temperature in toluene-d_8: (a) reaction mixture after 24 h reaction time in the absence of Cu(I)Br; (b) after addition of Cu(I)Br and a further 8 h reaction time.

Variation in the alkyl bromide component is also tolerated by the reaction (Table 4). Benzotriazole **1** and benzamide **40** react smoothly with substituted benzyl bromides **41**-**44** under the mild reaction conditions to form C–N coupled products **45**-**52**. Benzotriazole **1** also reacts productively with methyl 2-bromoacetate **58**, methyl 2-bromopropanoate **59**, 2-bromopropanenitrile **60,** 2-bromo-1-phenylethan-1-one **61** and 2-bromo-*N*-phenylpropanamide **62** to form coupled products **53**-**57**. These latter bromides do not undergo productive C–N couplings with the less reactive benzamide **40** under the standard conditions.

Table 4. [(PMDETA)Cu^{I}Br]-catalyzed alkylations of benzotriazole **1** and benzamide **40** with various alkyl bromides.

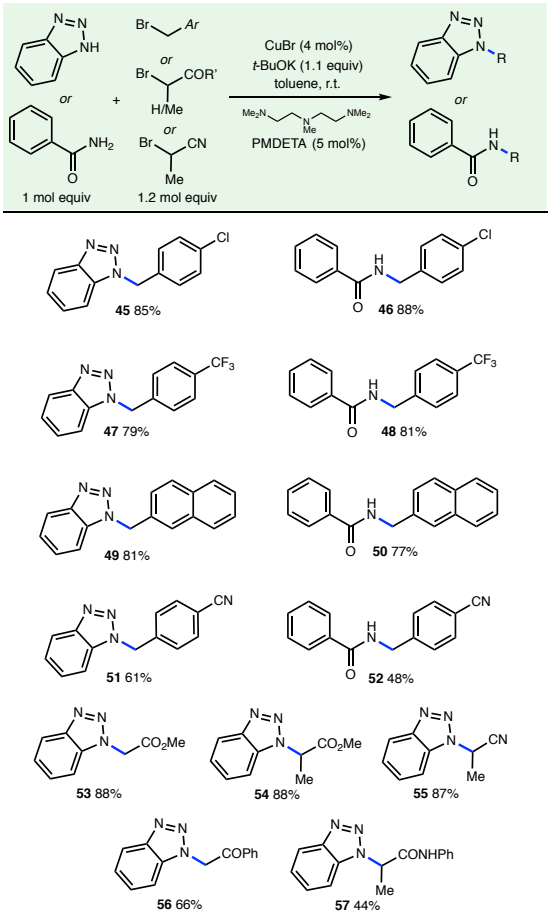

The use of ATRP-based activation methods offers new modes of reactivity and selectivity in cross-coupling reactions. Thus, Scheme 5 demonstrates an interesting example of ligand-controlled selectivity in the C–N coupling of benzotriazole **1** with two closely related alkyl bromides **58** and **60**.

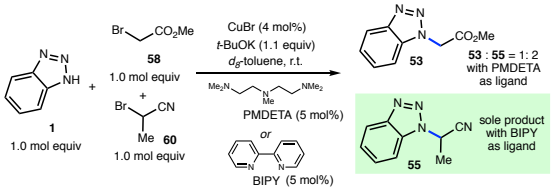

Scheme 4. Ligand-controlled selectivity in C–N couplings.

These reactions were monitored by ^{1}H NMR spectroscopy (stack plots are provided in the SI).

When the reactants were mixed under the usual conditions but with the omission of Cu(I)Br, no reaction took place over 24 h. After addition of Cu(I)Br and a further 8 h reaction time, smooth conversion to C–N coupled products was seen. With PMDETA as ligand, a mixture of the two possible products **53** and **55** was obtained. Using the less activating (Figure 1) BIPY ligand, however, only the more substituted bromide **60** couples, generating **55** as the sole product. We ascribe this outcome to a selective ISET reaction (Scheme 4) between the weaker [(BIPY)Cu(I)Br] ATRP catalyst and the more easily reduced bromide. Attempts to investigate the selectivity of the corresponding S_N2 reaction, by heating a reaction mixture of the same precursors in the absence of Cu(I)Br and PMDETA, were thwarted by the generation of a complex product mixture.

SUMMARY AND CONCLUSION

In summary, an operationally simple, room temperature, photochemistry-free, Cu(I)-catalyzed C–N coupling reaction has been developed. The process, which is uses an inexpensive (ATRP) precatalyst and ligand, proceeds via a novel Cu(I)→ Cu(II)→Cu(III)→Cu(I) catalytic cycle.

In line with other, recently reported Cu(I)-catalyzed methods (Scheme 1), the reaction is currently limited to activated C–Cl and C–Br bonds (i.e. those carrying an aryl-, acyl- or cyano-substituent). This reactivity profile is consistent with previous studies of R-X activation in the context of ATRP.[26] To date, for Cu catalysts, only photoredox processes have succeeded for non-activated bonds at room temperature. However, considerably more active ligands for ATRP catalysts are in development (Figure 1).[11] Thus further improvements toward non-activated bonds could be envisaged.

Despite the limitations summarized above, the substrate scope of this method is broader than the non-photochemical processes recently reported by Nishikata[5] and Fu,[6] which are limited to 2-halo-amides (Scheme 1). Moreover, since ATRP catalyst activity can be tuned over 7 orders of magnitude by simply by changing the ligand, this technique has the potential to selectively activate specific C–X bonds within a substrate. These studies and ligand-controlled enantioselective C–N couplings are currently under investigation.

EXPERIMENTAL SECTION

General Information. The starting materials were purchased from commercial suppliers and were used as received. Toluene was dried according to the procedure outlined by Grubbs and co-workers.[28] Analytical thin layer chromatography (TLC) was performed on aluminium-backed 0.2 mm thick silica gel 60 F254 plates and visualized by exposure to UV light (254 nm) and by staining with potassium permanganate : potassium carbonate : 5% sodium hydroxide aqueous solution : water (3 g : 20 g: 5mL : 300 mL) followed by heating. Flash chromatographic separations were carried out with silica gel 60 (40–63 µm) as the stationary phase using the laboratory grade solvents indicated. Proton (^{1}H) and proton-decoupled carbon ($^{13}C^{24}$) and APT ^{13}C NMR spectra were recorded at room temperature in $CDCl_3$ on a spectrometer operating at 400 MHz for proton and 100 MHz for carbon nuclei. ^{1}H NMR data are recorded as follows: chemical shift (δ) [multiplicity, coupling constant(s) J(Hz), relative integral] where multiplicity is defined as: s = singlet; d = doublet; t = triplet; q = quartet; m = multiplet or combinations thereof. The signal due to residual $CHCl_3$ appearing at δ_H = 7.26 ppm and the central resonance of the $CDCl_3$ 1:1:1 triplet appearing at δ_C = 77.16 ppm were used to reference ^{1}H and ^{13}C NMR spectra, respectively. Low resolution ESI mass spectra were recorded on a single quadrupole liquid chromatograph-mass spectrometer, while high resolution measurements were conducted on a time-of-flight instrument. Low and high resolution EI mass spectra were recorded on a magnetic sector machine.

General Experimental Procedure. To a flask containing copper (I) bromide (3.0 mg, 0.021 mmol), potassium *tert*-butoxide (62 mg, 0.55 mmol), and amine or amide (0.50 mmol) under dry N_2 was added toluene (1.2 mL), then PMDETA (0.050 mL, 0.024 mmol). The alkyl halide (0.60 mmol) was added dropwise over 90 mins, and the reaction mixture was stirred for 8 h at ambient temperature. After dilution with EtOAc (30 mL), the solution was washed with water (10 mL x 3) then dried over anhydrous sodium sulfate and concentrated under reduced pressure. The residue is purified by column chromatography using the solvent system indicated.

1-Benzyl-1*H*-benzo[1,2,3]triazole **3**

Relative amounts of precatalyst, ligand and amine shown in Table 1, entry 6 were used. Column chromatography was performed with EtOAc : *n*-hexane (1 : 9). Synthesis from benzyl chloride: colorless needles (0.098 g, 94%) Synthesis from benzyl bromide: white powder (0.097 g, 93%) **^{1}H NMR** (400 MHz, $CDCl_3$) *δ*/ppm 7.99 (d, *J* = 8.2 Hz, 1H), 7.61 – 6.95 (m, 8H), 5.76 (s, 2H). **^{13}C{^{1}H} NMR** (100 MHz, $CDCl_3$) *δ*/ppm 146.5, 134.9, 133.0, 129.1, 128.6, 127.7, 127.5, 124.0, 120.2, 109.9, 52.4. **MS** (ESI, +ve) *m/z* 232.1[(M+Na)$^+$, 100%]. **HRMS** *m/z* 210.1023 [M+H]$^+$ (calcd for $C_{13}H_{12}N_3$, 210.1031). Data are consistent with those reported in the literature.[29]

Larger scale (10 mmol) preparation of 1-benzyl-1*H*-benzo[1,2,3]triazole 3. To a flask containing copper (I) bromide (71 mg, 0.50 mmol), potassium *tert*-butoxide (1.23 g, 11 mmol), and benzotriazole (1.20 g, 10 mmol) under dry N_2 was added toluene (12 mL) then PMDETA (0.15 ml, 0.75 mmol). Benzyl chloride (1.15 ml, 10 mmol) was then added dropwise and the reaction mixture was stirred for 8 h at ambient temperature. Methanol (100 mL) and silica gel (125 mL) were added before evaporation under reduced pressure. The residue was loaded onto a silica gel column eluting with ethyl acetate : n-hexane (1 : 4) to give 1-benzyl-1*H*-benzo[1,2,3]triazole **3** as a white powder (1.71 g, 82%).

1-(1-Phenylethyl)-1*H*-benzo-1,2,3-triazole **24**
Column chromatography was performed with EtOAc : *n*-hexane (1 : 9) to give the product as a colorless needles (0.095 g, 85%). **^{1}H NMR** (400 MHz, $CDCl_3$) *δ*/ppm 8.25 (dd, *J* = 4.7, 1.6 Hz, 1H), 7.82 (dd, *J* = 7.8, 1.6 Hz, 1H), 7.30 – 7.14 (m, 5H), 6.98 (dd, *J* = 7.8, 4.7 Hz, 1H), 6.39 (d, *J* = 3.6 Hz, 1H), 6.26 (q, *J* = 7.2 Hz, 1H), 1.82 (d, *J* = 7.1 Hz, 3H). **^{13}C APT NMR** *δ*/ppm 147.5, 142.9, 142.4, 128.7, 127.6, 126.6, 125.3, 120.8, 116.0, 100.1, 52.0, 21.0. **MS** (ESI, +ve) *m/z* 224.1 [(M+H)$^+$, 100%]. **HRMS** *m/z* 224.1180 [M+H]$^+$ (calcd for $C_{14}H_{14}N_3$, 224.1188). Data are consistent with those reported in the literature.[30]

1-Benzyl-1*H*-pyrrolo[2,3-b]pyridine **25**
Column chromatography was performed with EtOAc : *n*-hexane (1 : 9). Synthesis from benzyl chloride: pale yellow oil (0.049 g, 47%). Synthesis from benzyl bromide: pale yellow oil (0.060 g, 58%). **^{1}H NMR** (400 MHz, $CDCl_3$) *δ*/ppm 8.03 (d, *J* = 7.5 Hz, 1H), 7.91 – 7.78 (m, 1H), 7.48 (d, *J* = 6.3 Hz, 1H), 7.34 – 7.24 (m, 5H), 6.77 (m, 1H), 6.64 (m, 1H), 5.84 (s, 2H). **^{13}C{^{1}H} NMR** (100 MHz, $CDCl_3$) *δ*/ppm 147.8, 143.1, 137.9, 128.9, 128.8, 128.0, 127.7, 127.6, 120.6, 116.0, 100.2, 47.9. **MS** (ESI, +ve) *m/z* 231 [(M+Na)$^+$, 100%]. **HRMS** *m/z* 209.1077 [M+H]$^+$ (calcd for $C_{14}H_{13}N_2$, 209.1079). Data are consistent with those reported in the literature.[31]

1-(1-Phenylethyl)-1*H*-pyrrolo[2,3-b]pyridine **26**
Column chromatography was performed with EtOAc : *n*-hexane (1 : 9) to give the product as a pale yellow powder (0.060 g, 54%). **^{1}H NMR** (400 MHz, $CDCl_3$) *δ*/ppm 8.24 (dd, *J* = 4.7, 1.6 Hz, 1H), 7.80 (dd, *J* = 7.8, 1.6 Hz, 1H), 7.32 – 7.06 (m, 5H), 6.96 (dd, *J* = 7.8, 4.7 Hz, 1H), 6.38 (d, *J* = 3.6 Hz, 1H), 6.24 (d, *J* = 7.2 Hz, 1H), 1.84 – 1.76 (m, 3H). **^{13}C{^{1}H} NMR** (100 MHz, $CDCl_3$) *δ*/ppm 147.5, 142.8, 142.4, 129.0, 128.7, 127.6, 126.6, 125.3, 120.8, 116.0, 100.1, 52.1, 21.0. **MS** (ESI, +ve) *m/z* 223.1 [(M+H)$^+$, 100%]. **HRMS** *m/z* 245.1059 [M+Na]$^+$ (calcd for $C_{15}H_{14}N_2Na$, 245.1055. Data are consistent with those reported in the literature.[32]

4-Benzyl-4*H*-1,2,4-triazole **27**
Column chromatography was performed with EtOAc : *n*-hexane (1 : 4). Synthesis from benzyl chloride: white solid (0.061 g, 77%). Synthesis from benzyl bromide: white solid (0.068 g 85%). **^{1}H NMR** (400 MHz, $CDCl_3$) *δ*/ppm 7.99 (s, 1H), 7.90 (s, 1H), 7.48 – 7.08 (m, 5H), 5.27 (s, 2H). **^{13}C APT NMR** (100 MHz, $CDCl_3$) *δ*/ppm 152.2, 134.5, 129.1, 128.7, 128.0, 53.6. **MS** (ESI, +ve) *m/z* 160.1 [(M+H)$^+$, 100%]. **HRMS** *m/z* 160.0864 [M+H]$^+$ (calcd for $C_9H_{10}N_3$, 160.0874). Data are consistent with those reported in the literature[31, 33]

4-(1-Phenylethyl)-4*H*-1,2,4-triazole **28**
Column chromatography was performed with EtOAc : *n*-hexane (3 : 7) to give the product as a white solid (0.076 g, 88%). **^{1}H NMR** (400 MHz, $CDCl_3$) *δ*/ppm 8.03 – 7.81 (m, 2H), 7.38 – 7.06 (m, 5H), 5.47 (q, *J* = 6.8 Hz, 1H), 1.85 (d, *J* = 7.0 Hz, 3H) **^{13}C{^{1}H} NMR** (100 MHz, $CDCl_3$) *δ*/ppm 151.9, 140.0, 129.0, 128.5, 126.5, 59.7, 21.3. **MS** (ESI, +ve) *m/z* 196.1 [(M+Na)$^+$, 100%]. **HRMS** *m/z* 196.0852 [M+Na]$^+$ (calcd for $C_{10}H_{11}N_3Na$, 196.0851). Data are consistent with those reported in the literature.[34]

1-Benzyl-3,5-dimethyl-1*H*-pyrazole **29**
Column chromatography was performed with EtOAc : *n*-hexane (1 : 9). Synthesis from benzyl chloride: white powder (0.080 g, 86%). Synthesis from benzyl bromide: white powder (0.078 g,

84%). **^{1}H NMR** (400 MHz, $CDCl_3$) δ/ppm 7.32 – 7.13 (m, 3H), 6.98 (d, *J* = 7.3 Hz, 2H), 5.77 (s, 1H), 5.13 (s, 2H), 2.16 (s, 3H), 2.05 (s, 3H). **^{13}C APT NMR** (100 MHz, $CDCl_3$) δ/ppm 147.6, 139.30, 137.4, 128.7, 127.4, 126.6, 105.7, 52.6, 13.5, 11.1. **MS** (ESI, +ve) *m/z* 187.1 [(M+H)$^+$, 100%]. **HRMS** *m/z* 187.1224 [M+H]$^+$ (calcd for $C_{12}H_{15}N_2$, 187.1235). Data are consistent with those reported in the literature.[35]

3,5-Dimethyl-1-(1-phenylethyl)-1*H*-pyrazole **30**
Column chromatography was performed with EtOAc : *n*-hexane (1 : 4) to give the product as a white solid (0.083 g, 83%). **^{1}H NMR** (400 MHz, $CDCl_3$) δ/ppm 7.24 – 7.09 (m, 3H), 7.04 – 6.99 (m, 2H), 5.74 (s, 1H), 5.26 (q, *J* = 7.1 Hz, 1H), 2.20 (s, 3H), 2.00 (s, 3H), 1.82 (d, *J* = 7.0 Hz, 3H). **^{13}C APT NMR** (100 MHz, $CDCl_3$) δ/ppm 147.1, 143.1, 139.1, 128.9, 127.7, 127.1, 125.7, 116.4, 55.0, 22.3, 13.4. **MS** (ESI, +ve) *m/z* 223.1 [M+Na]$^+$, 100%]. **HRMS** *m/z* 201.1383 [M+H]$^+$ (calcd for $C_{13}H_{17}N_2$, 201.1391). Data are consistent with those reported in the literature.[36]

9-Benzylcarbazole **31**
Column chromatography was performed with EtOAc : *n*-hexane (1 : 9). Synthesis from benzyl chloride: colorless plates (0.100 g, 78%). Synthesis from benzyl bromide: white solid (0.080 g, 62%). **^{1}H NMR** (400 MHz, $CDCl_3$) δ/ppm 8.02 (d, *J* = 7.6 Hz, 2H), 7.45 – 6.89 (m, 11H), 5.35 (s, 2H). **^{13}C{^{1}H} NMR** (100 MHz, $CDCl_3$) δ/ppm 140.7, 137.3, 128.8, 127.5, 126.5, 125.9, 123.1, 120.5, 119.3, 109.0, 46.6. **MS** (ESI, +ve) *m/z* 258.1 [(M+H)$^+$, 100%]. **HRMS** *m/z* 258.1287 [M+H]$^+$ (calcd for $C_{19}H_{16}N$, 258.1283). Data are consistent with those reported in the literature.[37]

9-(1-Phenylethyl)-9*H*-carbazole **6**
Column chromatography was performed with EtOAc : *n*-hexane (1 : 9) to give the product as a colorless plates (0.091 g, 67%). **^{1}H NMR** (400 MHz, $CDCl_3$) δ/ppm 8.01 (d, *J* = 7.7 Hz, 2H), 7.36 – 6.96 (m, 11H), 5.95 (q, *J* = 7.1 Hz, 1H), 1.87 (d, *J* = 7.1 Hz, 3H). **^{13}C{^{1}H} NMR** (100 MHz, $CDCl_3$) δ/ppm 140.8, 139.9, 128.7, 127.4, 126.6, 125.5, 123.5, 120.4, 119.0, 110.2, 52.4, 17.5. **MS** (ESI, +ve) *m/z* 272.1 [(M+H)$^+$, 100%]. **HRMS** *m/z* 272.1430 [M+H]$^+$ (calcd for $C_{20}H_{18}N$, 272.1439). Data are consistent with those reported in the literature.[38]

1-Benzyl-2-methyl-1*H*-imidazole **32**
Column chromatography was performed with EtOAc : *n*-hexane (3 : 7). Synthesis from benzyl chloride: appearance (0.076 g, 89%). Synthesis from benzyl bromide: appearance (0.078 g, 90%). **^{1}H NMR** (400 MHz, $CDCl_3$) δ/ppm 7.27 – 6.70 (m, 7H), 4.96 (s, 2H), 2.24 (s, 3H). **^{13}C APT NMR** (100 MHz, $CDCl_3$) δ/ppm 136.5, 128.9, 127.9, 127.4, 126.6, 49.8, 13.1. **MS** (ESI, +ve) *m/z* 195.1 [(M+Na)$^+$, 100%]. **HRMS** *m/z* 173.1071 [M+H]$^+$ (calcd for $C_{11}H_{13}N_2$, 173.1078). Data are consistent with those reported in the literature.[39]

2-Methyl-1-(1-phenylethyl)-1*H*-imidazole **33**
Column chromatography was performed with EtOAc : *n*-hexane (1 : 4) to give the product as a colorless oil (0.085 g, 91%). **^{1}H NMR** (400 MHz, $CDCl_3$) δ/ppm 7.31 – 7.14 (m, 3H), 6.94 (m, 4H), 5.21 (q, *J* = 6.7 Hz, 1H), 2.20 (q, *J* = 3.3 Hz, 3H), 1.73 (d, *J* = 5.8 Hz, 3H). **^{13}C APT NMR** (100 MHz, $CDCl_3$) δ/ppm 144.9, 141.8, 129.0, 127.8, 127.2, 125.8, 116.5, 55.1, 22.4, 13.5. **MS** (ESI, +ve) *m/z* 209.1 [(M+Na)$^+$, 100%]. **HRMS** *m/z* 187.1227 [M+H]$^+$ (calcd for $C_{12}H_{15}N_2$, 187.1235). Data are consistent with those reported in the literature.[40]

N-Benzylbenzamide **34**
Column chromatography was performed with EtOAc : *n*-hexane (2 : 3). Synthesis from benzyl chloride: white solid (0.088 g, 83%). Synthesis from benzyl bromide: white solid (0.081 g, 77%). **^{1}H NMR** (400 MHz, $CDCl_3$) δ/ppm 7.91 – 7.49 (m, 2H), 7.49 – 7.10 (m, 8H), 6.66 (s, 1H), 4.51 (d, *J* = 5.9 Hz, 2H). **^{13}C{^{1}H} NMR** (100 MHz, $CDCl_3$) δ/ppm 167.6, 138.4, 134.5, 131.6, 128.8, 128.6, 128.0, 127.6, 127.1, 44.2. **MS** (ESI, +ve) *m/z* 234.1 [(M+Na)$^+$, 100%]. **HRMS** *m/z* 212.1093 [M+H]$^+$ (calcd for $C_{14}H_{14}NO$, 212.1075). Data are consistent with those reported in the literature.[41]

N-(1-Phenylethyl)benzamide **35**
Column chromatography was performed with EtOAc : *n*-hexane (1 : 4) to give the product as a white solid (0.108 g, 96%). **^{1}H NMR** (400 MHz, $CDCl_3$) δ/ppm 7.73 – 7.65 (m, 2H), 7.46 – 7.07 (m, 8H), 6.40 (d, *J* = 7.5 Hz, 1H), 5.25 (p, *J* = 7.1 Hz, 1H), 1.51 (d, *J* = 6.9 Hz, 3H). **^{13}C{^{1}H} NMR** (100 MHz, $CDCl_3$) δ/ppm 166.6, 143.2, 134.6, 131.5, 128.8, 128.6, 127.5, 127.0, 126.3, 49.2, 21.8. **MS** (ESI, +ve) *m/z* 248.1 [(M+Na)$^+$, 100%]. **HRMS** *m/z* 248.1051 [M+Na]$^+$ (calcd for $C_{15}H_{15}NNaO$, 248.1051). Data are consistent with those reported in the literature.[42]

1-Benzylpyrrolidin-2-one **36**
Column chromatography was performed with EtOAc. Synthesis from benzyl chloride: colourless oil (0.077 g, 88%). Synthesis from benzyl bromide: colorless oil (0.076 g, 87%). **^{1}H NMR** (400 MHz,

$CDCl_3$) δ/ppm 7.35 – 7.09 (m, 5H), 4.38 (s, 2H), 3.18 (t, J = 7.1 Hz, 2H), 2.36 (t, J = 8.1 Hz, 2H), 2.03 – 1.81 (m, 2H). **$^{13}C\{^1H\}$ NMR** (100 MHz, $CDCl_3$) δ/ppm 175.0, 136.7, 128.7, 128.2, 127.6, 46.7, 46.7, 31.0, 17.8. , 17.7. **MS** (ESI, +ve) *m/z* 198.1 [(M+Na)$^+$, 100%]. **HRMS** *m/z* 198.0909 [M+Na]$^+$ (calcd for $C_{11}H_{13}NNaO$, 198.0895). Data are consistent with those reported in the literature.[42]

1-(1-Phenylethyl)pyrrolidin-2-one **37**
Column chromatography was performed with EtOAc : *n*-hexane (3 : 7) to give the product as a colorless plates (0.079 g, 84%). **^1H NMR** (400 MHz, $CDCl_3$) δ/ppm 7.22 (m, 5H), 5.41 (q, J = 7.1 Hz, 1H), 3.36 – 3.17 (m, 1H), 2.90 (m, 1H), 2.50 – 2.26 (m, 2H), 1.84 (m, 2H), 1.44 (d, J = 7.1 Hz, 3H). **$^{13}C\{^1H\}$ NMR** (100 MHz, $CDCl_3$) δ/ppm 174.4, 140.3, 128.5, 127.4, 127.0, 48.9, 42.3, 31.4, 17.9, 16.2. **MS** (ESI, +ve) *m/z* 212.1 [(M+Na)$^+$, 100%]. **HRMS** *m/z* 212.1045 [M+Na]$^+$ (calcd for $C_{12}H_{15}NNaO$, 212.1051). Data are consistent with those reported in the literature.[42]

1-(4-Chlorobenzyl)-1*H*-benzo[d][1,2,3]triazole **45**
Column chromatography was performed with EtOAc : *n*-hexane (3 : 7) to give the product as a colorless needles (0.104 g, 85%). **^1H NMR** (400 MHz, $CDCl_3$) δ/ppm 8.00 (d, J = 8.3 Hz, 1H), 7.50 – 7.21 (m, 5H), 7.13 (d, J = 8.4 Hz, 2H), 5.74 (s, 2H). **$^{13}C\{^1H\}$ NMR** (100 MHz, $CDCl_3$) δ/ppm 146.5, 134.7, 133.4, 132.8, 129.4, 129.1, 127.8, 124.2, 120.4, 109.6, 51.7. **MS** (ESI, +ve) *m/z* 266.0 [(M+Na)$^+$, 100%]. **HRMS** *m/z* 266.0465 [M(^{35}Cl)+Na]$^+$ (calcd for $C_{13}H_{10}{}^{35}ClN_3Na$, 266.0461). Data are consistent with those reported in the literature.[43]

N-(4-Chlorobenzyl)benzamide **46**
Column chromatography was performed with EtOAc : *n*-hexane (3 : 7) to give the product as a white solid (0.108 g, 88%). **^1H NMR** (400 MHz, $CDCl_3$) δ/ppm 7.69 (dd, J = 7.1, 1.7 Hz, 2H), 7.41 (td, J = 7.3, 1.7 Hz, 1H), 7.31 (td, J = 7.5, 1.7 Hz, 2H), 7.17 (tdd, J = 8.5, 6.3, 3.0 Hz, 4H), 6.71 (s, 1H), 4.55 – 4.37 (m, 2H). **$^{13}C\{^1H\}$ NMR** (100 MHz, $CDCl_3$) δ/ppm 166.5, 135.8, 133.1, 132.2, 130.6, 128.1, 127.7, 127.6, 126.0, 42.3. **MS** (ESI, +ve) *m/z* 268.1 [(M(^{35}Cl)+Na)$^+$, 100%]. **HRMS** *m/z* 268.0536 [M(^{35}Cl)+Na]$^+$ (calcd for $C_{14}H_{12}{}^{35}ClNONa$, 268.0505). Data are consistent with those reported in the literature.[44]

1-(4-(Trifluoromethyl)benzyl)-1H-benzo[d][1,2,3] triazole **47**
Column chromatography was performed with EtOAc : *n*-hexane (2 : 8) to give the product as a white solid (0.110 g, 79%). **^1H NMR** (400 MHz, $CDCl_3$) δ/ppm 8.00 (d, J = 8.1 Hz, 1H), 7.50 (d, J = 8.1 Hz, 2H), 7.41 – 7.24 (m, 5H), 5.82 (s, 2H). **$^{13}C\{^1H\}$ NMR** (100 MHz, $CDCl_3$) δ/ppm 146.5 , 138.9 (d, $^2J_{C\text{-}F}$ = 1.8 Hz), 132.9 , 130.9 (q, $^1J_{C\text{-}F}$ = 32.7 Hz), 127.9 , 127.9 , 126.2 (q, ^2J = 3.7 Hz), 124.3, 123.9 (q, ^3J = 272.3 Hz), 120.4 , 109.5 , 51.6 **MS** (ESI, +ve) *m/z* 300.1 [(M+Na)$^+$, 100%]. **HRMS** *m/z* 278.0911 [M+H]$^+$ (calcd for $C_{14}H_{11}N_3F_3$, 278.0905). Data are consistent with those reported in the literature.[45]

N-(4-(Trifluoromethyl)benzyl)benzamide **48**
Column chromatography was performed with EtOAc : *n*-hexane (2 : 8) to give the product as a colorless needles (0.113 g, 81%). **^1H NMR** (400 MHz, $CDCl_3$) δ/ppm 7.74 – 7.69 (m, 2H), 7.50 (d, J = 8.0 Hz, 2H), 7.46 – 7.40 (m, 1H), 7.35 (d, J = 8.1 Hz, 4H), 6.67 (t, J = 5.9 Hz, 1H), 4.59 (d, J = 6.0 Hz, 2H). **$^{13}C\{^1H\}$ NMR** (100 MHz, $CDCl_3$) δ/ppm 167.6, 142.4, 134.0, 131.8, 129.8 (q, $^1J_{C\text{-}F}$ = 32.3 Hz), 128.7, 127.9, 127., 125.7 (q, $^2J_{C\text{-}F}$ = 3.8 Hz), 122.7, 43.5. **MS** (ESI, +ve) *m/z* 302.1 [(M+Na)$^+$, 100%]. **HRMS** *m/z* 302.0772 [M+Na]$^+$ (calcd for $C_{15}H_{12}F_3NONa$, 302.0769). Data are consistent with those reported in the literature.[46]

1-(Naphthalen-2-ylmethyl)-1*H*-benzo[d][1,2,3] triazole **49**
Column chromatography was performed with EtOAc : *n*-hexane (2 : 8) to give the product as a white solid (0.105 g, 81%). **^1H NMR** (400 MHz, $CDCl_3$) δ/ppm 8.08 (d, J = 7.8 Hz, 1H), 7.87 – 7.72 (m, 4H), 7.53 – 7.46 (m, 2H), 7.36 (m, 4H), 6.00 (s, 2H). **$^{13}C\{^1H\}$ NMR** (100 MHz, $CDCl_3$) δ/ppm 146.4, 133.2, 133.1, 132.9, 132.2, 129.1, 127.9, 127.8, 127.5, 126.7, 126.7, 126.5, 125.0, 124.0, 120.1, 109.8, 52.5. **MS** (ESI, +ve) *m/z* 282.1 [(M+Na)$^+$, 100%]. **HRMS** *m/z* 282.1022 [M+Na]$^+$ (calcd for $C_{17}H_{13}N_3Na$, 282.1007).

N-(Naphthalen-2-ylmethyl)benzamide **50**
Column chromatography was performed with EtOAc : *n*-hexane (2 : 8) to give the product as a pale yellow solid (0.101 g, 77%). **^1H NMR** (400 MHz, $CDCl_3$) δ/ppm 7.91 – 7.74 (m, 6H), 7.62 – 7.34 (m, 6H), 6.63 (s, 1H), 4.79 (d, J = 5.7 Hz, 2H). **$^{13}C\{^1H\}$ NMR** (100 MHz, $CDCl_3$) δ/ppm 167.4, 135.7, 134.4, 133.4, 132.8, 131.6, 128.6, 127.8, 127.7, 127.0, 126.5, 126.3, 126.0, 126.0, 44.3. **MS** (ESI, +ve) *m/z* 284.1 [(M+Na)$^+$, 100%]. **HRMS** *m/z*

284.1063 $[M+Na]^+$ (calcd for $C_{18}H_{15}NONa$, 284.1051). Data are consistent with those reported in the literature.[47]

4-((1*H*-Benzo[d][1,2,3]triazol-1-yl)methyl) benzonitrile **51**

Column chromatography was performed with EtOAc : *n*-hexane (3 : 7) to give the product as a colorless needles (0.072 g, 61%). **^{1}H NMR** (400 MHz, $CDCl_3$) *δ*/ppm 8.04 (dd, *J* = 8.3, 1.1 Hz, 1H), 7.57 (d, *J* = 8.3 Hz, 2H), 7.44 – 7.37 (m, 2H), 7.33 – 7.25 (m, 3H), 5.84 (s, 2H) **^{13}C{^{1}H} NMR** (100 MHz, $CDCl_3$) *δ*/ppm 146.5, 140.1, 133.0, 132.9, 128.2, 128.2, 124.5, 120.6, 118.3, 112.8, 109.3, 51.6. **MS** (ESI, +ve) *m/z* 257.1 $[(M+Na)^+$, 100%]. **HRMS** *m/z* 257.0811 $[M+Na]^+$ (calcd for $C_{14}H_{10}NaN_4$, 257.0803). Data are consistent with those reported in the literature.[45]

N-(4-Cyanobenzyl)benzamide **52**

Preparative thin layer chromatography was performed with EtOAc : *n*-hexane (3 : 7) to give the product as a colorless plates (0.057 g, 48%). **^{1}H NMR** (400 MHz, $CDCl_3$) *δ*/ppm 7.80 (d, *J* = 7.3 Hz, 2H), 7.62 (d, *J* = 8.1 Hz, 2H), 7.53 (d, *J* = 7.3 Hz, 1H), 7.45 (dd, *J* = 7.5, 5.2 Hz, 4H), 6.62 (m, 1H), 4.71 (s, 2H). **^{13}C{^{1}H} NMR** (100 MHz, $CDCl_3$) *δ*/ppm 167.7, 144.0, 133.9, 132.7, 132.1, 128.9, 128.4, 127.1, 118.8, 111.5, 43.7.. **MS** (ESI, +ve) *m/z* 259.1 $[(M+Na)^+$, 100%]. **HRMS** *m/z* 259.0861 $[M+Na]^+$ (calcd for $C_{15}H_{12}N_2ONa$, 259.0847). Data are consistent with those reported in the literature.[48]

2-(1*H*-Benzo-1,2,3-triazol-1-yl) propanenitrile **53**

Column chromatography was performed with EtOAc : *n*-hexane (4 : 6) to give the product as a yellow oil (0.076 g, 88%). **^{1}H NMR** (400 MHz, $CDCl_3$) *δ*/ppm 8.05 (d, *J* = 8.4 Hz, 1H), 7.67 – 7.63 (m, 1H), 7.53 (ddd, *J* = 8.3, 7.0, 1.0 Hz, 1H), 7.39 (ddd, *J* = 8.1, 7.0, 1.0 Hz, 1H), 5.94 (q, *J* = 7.3 Hz, 1H), 2.04 (d, *J* = 7.3 Hz, 3H). **^{13}C{^{1}H} NMR** (100 MHz, $CDCl_3$) *δ*/ppm 146.5, 131.4, 128.6, 124.9, 120.7, 115.9, 109.2, 45.1, 19.6. **MS** (ESI, +ve) *m/z* 195.1 $[(M+Na)^+$, 100%]. **HRMS** *m/z* 195.0650 $[M+Na]^+$ (calcd for $C_9H_8N_4Na$, 195.0646).

Methyl 2-(1*H*-benzo-1,2,3-triazol-1-yl)acetate **54**

Column chromatography was performed with EtOAc : *n*-hexane (4 : 6) to give the product as a white solid (0.084 g, 88%). **^{1}H NMR** (400 MHz, $CDCl_3$) *δ*/ppm 7.81 (dd, *J* = 6.6, 3.1 Hz, 2H), 7.34 (dd, *J* = 6.6, 3.1 Hz, 2H), 5.47 (s, 2H), 3.73 (s, 3H). **^{13}C{^{1}H} NMR** (100 MHz, $CDCl_3$) *δ*/ppm 166.6, 144.9, 126.9, 118.3, 57.00, 53.1. **MS** (ESI, +ve) *m/z* 214.0 $[(M+Na)^+$, 100%]. **HRMS** *m/z* 214.0589 $[M+Na]^+$ (calcd for $C_9H_9N_3NaO_2$, 214.0592). Data are consistent with those reported in the literature.[49]

Methyl 2-(1*H*-benzo[d][1,2,3]triazol-1-yl)propanoate **55**

Column chromatography was performed with EtOAc : *n*-hexane (4 : 6) to give the product as a white solid (0.089 g, 87%). **^{1}H NMR** (400 MHz, $CDCl_3$) *δ*/ppm 8.01 (d, *J* = 8.3 Hz, 1H), 7.49 – 7.38 (m, 2H), 7.31 (ddd, *J* = 8.1, 6.3, 1.6 Hz, 1H), 5.64 (q, *J* = 7.4 Hz, 1H), 3.66 (s, 3H), 1.96 (d, *J* = 7.6 Hz, 3H). **^{13}C{^{1}H} NMR** (100 MHz, $CDCl_3$) *δ*/ppm 169.7, 146.3, 132.5, 127.6, 124.1, 120.3, 109.9, 57.1, 53.0, 16.7. **MS** (ESI, +ve) *m/z* 228.1 $[(M+Na)^+$, 100%]. **HRMS** *m/z* 228.0744 $[M+Na]^+$ (calcd for $C_{10}H_{11}N_3O_2Na$, 228.0749).

2-(1*H*-Benzo[d][1,2,3]triazol-1-yl)-1-phenylethan-1-one **56**

Column chromatography was performed with EtOAc : *n*-hexane (2 : 8) to give the product as a white solid (0.094 g, 66%). **^{1}H NMR** (400 MHz, $CDCl_3$) *δ*/ppm 8.01 (d, J = 8.0 Hz, 2H), 7.90 (d, J = 7.7 Hz, 2H), 7.66 (t, J = 7.4 Hz, 1H), 7.53 (t, J = 7.3 Hz, 2H), 7.41 (d, J = 7.7 Hz, 2H), 6.20 (s, 2H). **^{13}C{^{1}H} NMR** (100 MHz, $CDCl_3$) *δ*/ppm 190.4, 145.1, 134.5, 134.4, 129.2, 128.8, 128.6, 128.3, 126.9, 126.9, 118.4, 62.0. **MS** (ESI, +ve) *m/z* 238.1 $[(M+H)^+$, 100%]. **HRMS** *m/z* 260.0788 $[M+Na]^+$ (calcd for $C_{14}H_{11}N_3ONa$, 260.0800) Data are consistent with those reported in the literature.[50]

2-(1*H*-Benzo[d][1,2,3]triazol-1-yl)-N-phenylpropanamide **57**

Column chromatography was performed with EtOAc : *n*-hexane (2 : 8) to give the product as a white solid (0.062 g, 44%). **^{1}H NMR** (400 MHz, $CDCl_3$) *δ*/ppm 8.43 (s, 1H), 7.93 (dd, J = 6.6, 3.0 Hz, 2H), 7.52 – 7.41 (m, 4H), 7.29 (t, J = 7.8 Hz, 2H), 7.11 (t, J = 7.4 Hz, 1H), 5.76 (q, J = 7.3 Hz, 1H), 2.11 (d, J = 7.3 Hz, 3H). **^{13}C{^{1}H} NMR** (100 MHz, $CDCl_3$) *δ*/ppm 166.1, 144.7, 137.0, 129.2, 127.5, 125.1, 120.3, 118.4, 66.6, 18.9. **MS** (ESI, +ve) *m/z* 267.1 $[(M+H)^+$, 100%]. **HRMS** *m/z* 267.1251 $[M+H]^+$ (calcd for $C_{10}H_{15}N_4O$, 267.1246).

Computational Methods. All geometry optimizations, frequency calculations and single point energy calculations were performed using Gaussian 16 software package.[51] The level of theory used in the current study is based on that previously benchmarked for the initial ISET reaction,[25] the only change being the use of

solution-phase optimized geometries in the present work in place of gas-phase optimized geometries. Geometries were optimized in solution with ω-B97XD functional and a mixed basis set of SDD [52] for Cu and 6-31G(d)[53] for other atoms (denoted as Basis-set-1). Single point energies were calculated using ω-B97XD functional with Def2TZVP basis set[54] in toluene using CPCM solvation model[55] for higher-level electronic energy correction. Reported Gibbs free energies in solution at 298K were calculated using the direct method[56, 57] based on solution phase optimized geometries, including zero-point correction, thermal corrections and entropy calculated at ω-B97XD/Basis-set-1 and electronic energy calculated at ω-B97XD/Def2TZVP. The activation free energy for the outer-sphere single electron transfer reaction was calculated using Marcus theory[58, 59] (see the Supporting Information for more details). Detailed results and discussion, including reaction energetics, total energies of all species and optimized geometries are provided in Section S2 of the Supporting Information.

CONFLICTS OF INTEREST

There are no conflicts to declare.

Funding Sources

Australian Research Council (FL170100041, CE140100012, DP160104322).

ASSOCIATED CONTENT

Supporting Information

The Supporting Information is available free of charge at https://pubs.acs.org/XXXX.

General experimental details, ^{1}H, ^{13}C{^{1}H} and ^{13}C APT NMR spectra, computational details including Gaussian archive files for gas-phase geometries (PDF)

ACKNOWLEDGEMENTS

MLC gratefully acknowledges financial support from the Australian Research Council (ARC) Centre of Excellence for Electromaterials Science, an ARC Laureate Fellowship, and generous supercomputing time from the National Computational Infrastructure, and useful discussions with Professor Martin Banwell and Dr Philip Norcott. AKKF thanks Dr. Benjamin Noble, for his guidance and advice. MSS gratefully acknowledges financial support from the Australian Research Council (ARC) for Discovery Grant DP160104322.

NOTES AND REFERENCES

1. Bariwal, J.; Van der Eycken, E., C–N bond forming cross-coupling reactions: an overview. *Chem. Soc. Rev.* **2013,** *42*, 9283-9303.
2. Ahn, J. M.; Peters, J. C.; Fu, G. C., Design of a Photoredox Catalyst that Enables the Direct Synthesis of Carbamate-Protected Primary Amines via Photoinduced, Copper-Catalyzed N-Alkylation Reactions of Unactivated Secondary Halides. *J. Am. Chem. Soc.* **2017,** *139*, 18101-18106.
3. Liang, Y.; Zhang, X.; MacMillan, D. W. C., Decarboxylative sp3 C–N coupling via dual copper and photoredox catalysis. *Nature* **2018,** *559*, 83-88.
4. Shafir, A.; Buchwald, S. L., Highly Selective Room-Temperature Copper-Catalyzed C−N Coupling Reactions. *J. Am. Chem. Soc.* **2006,** *128*, 8742-8743.
5. Ishida, S.; Takeuchi, K.; Taniyama, N.; Sunada, Y.; Nishikata, T., Copper-Catalyzed Amination of Congested and Functionalized α-Bromocarboxamides with either Amines or Ammonia at Room Temperature. *Angew. Chem. Int. Ed.* **2017,** *56*, 11610-11614.
6. Bartoszewicz, A.; Matier, C. D.; Fu, G. C., Enantioconvergent Alkylations of Amines by Alkyl Electrophiles: Copper-Catalyzed Nucleophilic Substitutions of Racemic α-Halolactams by Indoles. *J. Am. Chem. Soc.* **2019,** *141*, 14864-14869.
7. Kato, M.; Kamigaito, M.; Sawamoto, M.; Higashimura, T., Polymerization of Methyl Methacrylate with the Carbon Tetrachloride/Dichlorotris-(triphenylphosphine)ruthenium(II)/Methylaluminum Bis(2,6-di-tert-butylphenoxide) Initiating System: Possibility of Living Radical Polymerization. *Macromolecules* **1995,** *28*, 1721-1723.
8. Wang, J.-S.; Matyjaszewski, K., Controlled/"living" radical polymerization. atom transfer radical polymerization in the presence of transition-metal complexes. *J. Am. Chem. Soc.* **1995,** *117*, 5614-5615.
9. Kharasch, M. S.; Jensen, E. V.; Urry, W. H., Addition of carbon tetrachloride and chloroform to olefins. *Science* **1945,** *102*, 128-128.
10. Ribelli, T. G.; Fantin, M.; Daran, J.-C.; Augustine, K. F.; Poli, R.; Matyjaszewski, K., Synthesis and Characterization of the Most Active Copper ATRP Catalyst Based on Tris[(4-dimethylaminopyridyl)methyl]amine. *J. Am. Chem. Soc.* **2018,** *140*, 1525-1534.
11. Doan, V.; Noble, B. B.; Fung, A. K. K.; Coote, M. L., Rational Design of Highly Activating Ligands for Cu-Based Atom Transfer Radical Polymerization. *J. Org. Chem.* **2019,** *84*, 15624-15632.
12. Enciso, A. E.; Lorandi, F.; Mehmood, A.; Fantin, M.; Szczepaniak, G.; Janesko, B. G.; Matyjaszewski, K., p - Substituted Tris(2 - pyridylmethyl)amines as Ligands for Highly Active ATRP Catalysts: Facile Synthesis and Characterization *Angew. Chem. Int. Ed.* **2020,** *132*, 15020-15030.
13. Tang, W.; Kwak, Y.; Braunecker, W.; Tsarevsky, N. V.; Coote, M. L.; Matyjaszewski, K., Understanding Atom Transfer Radical Polymerization: Effect of Ligand and Initiator Structures on the Equilibrium Constants. *J. Am. Chem. Soc.* **2008,** *130*, 10702-10713.
14. Xia, J.; Matyjaszewski, K., Controlled/"Living" Radical Polymerization. Atom Transfer Radical Polymerization Using Multidentate Amine Ligands. *Macromolecules* **1997,** *30*, 7697-7700.
15. Fung, A. K. K.; Coote, M. L., A Mechanistic Perspective on Atom Transfer Radical Polymerization. *Polym. Int.* **2021,** *70*, 918-926.
16. Rajakumar, P.; Murali, V.; Kalaivasan, N., Synthesis of intra annularly linked benzotriazolophane. *Synth. Commun.* **2002,** *32*, 1685-1690.

17. Fagel, J. E.; Ewing, G. W., The Ultraviolet Absorption of Benzotriazole. *J. Am. Chem. Soc.* **1951,** *73*, 4360-4362.
18. Konkolewicz, D.; Krys, P.; Góis, J. R.; Mendonça, P. V.; Zhong, M.; Wang, Y.; Gennaro, A.; Isse, A. A.; Fantin, M.; Matyjaszewski, K., Aqueous RDRP in the Presence of Cu0: The Exceptional Activity of CuI Confirms the SARA ATRP Mechanism. *Macromolecules* **2014,** *47*, 560-570.
19. Xiong, Y.; Zhang, G., Visible-Light-Induced Copper-Catalyzed Intermolecular Markovnikov Hydroamination of Alkenes. *Org. Lett.* **2019,** *21*, 7873-7877.
20. Xiao, E.-K.; Wu, X.-T.; Ma, F.; Feng, X.; Chen, P.; Jiang, Y.-J., Fe(OTf)3- and γ-Cyclodextrin-Catalyzed Hydroamination of Alkenes with Carbazoles. *Org. Lett.* **2021,** *23*, 449-453.
21. Dong, J.; Liu, Y.; Hu, J.; Baigude, H.; Zhang, H., A novel ferrocenyl-based multichannel probe for colorimetric detection of Cu(II) and reversible fluorescent "turn-on" recognition of Hg(II) in aqueous environment and living cells. *Sens. Actuators B Chem.* **2018,** *255*, 952-962.
22. Fantin, M.; Isse, A. A.; Gennaro, A.; Matyjaszewski, K., Understanding the Fundamentals of Aqueous ATRP and Defining Conditions for Better Control. *Macromolecules* **2015,** *48*, 6862-6875.
23. Matyjaszewski, K.; Paik, H.-j.; Shipp, D. A.; Isobe, Y.; Okamoto, Y., Free-Radical Intermediates in Atom Transfer Radical Addition and Polymerization: Study of Racemization, Halogen Exchange, and Trapping Reactions. *Macromolecules* **2001,** *34*, 3127-3129.
24. Sarbu, T.; Lin, K.-Y.; Ell, J.; Siegwart, D. J.; Spanswick, J.; Matyjaszewski, K., Polystyrene with Designed Molecular Weight Distribution by Atom Transfer Radical Coupling. *Macromolecules* **2004,** *37*, 3120-3127.
25. Fang, C.; Fantin, M.; Pan, X. C.; de Fiebre, K.; Coote, M. L.; Matyjaszewski, K.; Liu, P., Mechanistically Guided Predictive Models for Ligand and Initiator Effects in Copper-Catalyzed Atom Transfer Radical Polymerization (Cu-ATRP). *J. Am. Chem. Soc.* **2019,** *141*, 7486-7497.
26. Lin, C. Y.; Coote, M. L.; Gennaro, A.; Matyjaszewski, K., Ab initio evaluation of the thermodynamic and electrochemical properties of alkyl halides and radicals and their mechanistic implications for atom transfer radical polymerization. *J. Am. Chem. Soc.* **2008,** *130*, 12762-12774.
27. Jones, G. O.; Liu, P.; Houk, K. N.; Buchwald, S. L., Computational Explorations of Mechanisms and Ligand-Directed Selectivities of Copper-Catalyzed Ullmann-Type Reactions. *J. Am. Chem. Soc.* **2010,** *132*, 6205-6213.
28. Pangborn, A. B.; Giardello, M. A.; Grubbs, R. H.; Rosen, R. K.; Timmers, F. J., Safe and Convenient Procedure for Solvent Purification. *Organometallics* **1996,** *15*, 1518-1520.
29. Muraca, A. C. A.; Raminelli, C., Exploring Possible Surrogates for Kobayashi's Aryne Precursors. *ACS Omega* **2020,** *5*, 2440-2457.
30. Liu, W.; Liu, C.; Zhang, Y.; Sun, Y.; Abdukadera, A.; Wang, B.; Li, H.; Ma, X.; Zhang, Z., Reusable ionic liquid-catalyzed oxidative coupling of azoles and benzylic compounds via sp3 C–N bond formation under metal-free conditions. *Org. Biomol. Chem.* **2015,** *13*, 7154-7158.
31. Li, Z.; Dechantsreiter, M.; Dandapani, S., Systematic Investigation of the Scope of Transannular C–H Heteroarylation of Cyclic Secondary Amines for Synthetic Application in Medicinal Chemistry. *J. Org. Chem.* **2020,** *85*, 6747-6760.
32. Laha, J. K.; Bhimpuria, R. A.; Hunjan, M. K., Intramolecular Oxidative Arylations in 7-Azaindoles and Pyrroles: Revamping the Synthesis of Fused N-Heterocycle Tethered Fluorenes. *Chem. Eur. J.* **2017,** *23*, 2044-2050.
33. Hutchinson, S. M.; Ardón-Muñoz, L. G.; Ratliff, M. L.; Bolliger, J. L., Catalytic Preparation of 1-Aryl-Substituted 1,2,4-Triazolium Salts. *ACS Omega* **2019,** *4*, 17923-17933.
34. Keith, S.; Andrew, S.; G., H. M., Regiospecific Synthesis of 1-Substituted 1,2,4-Triazoles Involving Isomerization of the Corresponding 4-Substituted Compounds. *Chem. Lett.* **1990,** *19*, 347-350.
35. Schneider, Y.; Prévost, J.; Gobin, M.; Legault, C. Y., Diazirines as Potent Electrophilic Nitrogen Sources: Application to the Synthesis of Pyrazoles. *Organic Letters* **2014,** *16*, 596-599.
36. Gulia, N.; Daugulis, O., Palladium-Catalyzed Pyrazole-Directed sp3 C–H Bond Arylation for the Synthesis of β-Phenethylamines. *Angew. Chem. Int. Ed.* **2017,** *56*, 3630-3634.
37. Liu, L.; Tang, Y.; Wang, K.; Huang, T.; Chen, T., Transition-Metal-Free and Base-Promoted Carbon–Heteroatom Bond Formation via C–N Cleavage of Benzyl Ammonium Salts. *J. Org. Chem.* **2021,** *86*, 4159-4170.
38. Xiao, E.-K.; Wu, X.-T.; Ma, F.; Feng, X.; Chen, P.; Jiang, Y.-J., Fe(OTf)3- and γ-Cyclodextrin-Catalyzed Hydroamination of Alkenes with Carbazoles. *Organic Letters* **2021,** *23*, 449-453.
39. Chakraborty, A.; Debnath, S.; Ghosh, T.; Maiti, D. K.; Majumdar, S., An efficient strategy for N-alkylation of benzimidazoles/imidazoles in SDS-aqueous basic medium and N-alkylation induced ring opening of benzimidazoles. *Tetrahedron* **2018,** *74*, 5932-5941.
40. Maccallini, C.; Patruno, A.; Lannutti, F.; Ammazzalorso, A.; De Filippis, B.; Fantacuzzi, M.; Franceschelli, S.; Giampietro, L.; Masella, S.; Felaco, M., et al., N-Substituted acetamidines and 2-methylimidazole derivatives as selective inhibitors of neuronal nitric oxide synthase. *Bioorg. Med. Chem. Lett.* **2010,** *20*, 6495-6499.
41. Wang, Z.; Matsumoto, A.; Maruoka, K., Efficient cleavage of tertiary amide bonds via radical–polar crossover using a copper(ii) bromide/Selectfluor hybrid system. *Chem. Sci.* **2020,** *11*, 12323-12328.
42. Wang, G.-W.; Sokolova, O. O.; Young, T. A.; Christodoulou, E. M. S.; Butts, C. P.; Bower, J. F., Carbonylative C–C Bond Activation of Aminocyclopropanes Using a Temporary Directing Group Strategy. *J. Am. Chem. Soc.* **2020,** *142*, 19006-19011.
43. Chen, Q.; Yu, H.; Xu, Z.; Lin, L.; Jiang, X.; Wang, R., Development and Application of O-(Trimethylsilyl)aryl Fluorosulfates for the Synthesis of Arynes. *J. Org. Chem.* **2015,** *80*, 6890-6896.
44. Ghosh, C.; Kim, S.; Mena, M. R.; Kim, J.-H.; Pal, R.; Rock, C. L.; Groy, T. L.; Baik, M.-H.; Trovitch, R. J., Efficient Cobalt Catalyst for Ambient-Temperature Nitrile Dihydroboration, the Elucidation of a Chelate-Assisted Borylation Mechanism, and a New Synthetic Route to Amides. *J. Am. Chem. Soc.* **2019,** *141*, 15327-15337.
45. Ankati, H.; Biehl, E., Microwave-assisted benzyne-click chemistry: preparation of 1H-benzo[d][1,2,3]triazoles. *Tetrahedron Lett.* **2009,** *50*, 4677-4682.
46. Pandey, V. K.; Tiwari, C. S.; Rit, A., Silver-Catalyzed Hydroboration of C–X (X = C, O, N) Multiple Bonds. *Organic Letters* **2021,** *23*, 1681-1686.
47. Zhang, Q.; Li, J.; Li, J.; Yuan, S.; Li, D., An unprecedented cobalt-catalyzed selective aroylation of primary amines with aroyl peroxides. *Tetrahedron Lett.* **2020,** *61*, 152399.
48. Chen, Z.; Wen, X.; Zheng, W.; He, R.; Chen, D.; Cao, D.; Long, L.; Ye, M., Acyl Cyanides as Bifunctional Reagent: Application in Copper-Catalyzed Cyanoamidation and Cyanoesterification Reaction. *J. Org. Chem.* **2020,** *85*, 5691-5701.
49. Yang, Y.; Qin, A.; Zhao, K.; Wang, D.; Shi, X., Design and Synthesis of Alanine Triazole Ligands and Application in Promotion of Hydration, Allene Synthesis and Borrowing Hydrogen Reactions. *Adv. Synth. Catal.* **2016,** *358*, 1433-1439.
50. More, A. A.; Pathe, G. K.; Parida, K. N.; Maksymenko, S.; Lipisa, Y. B.; Szpilman, A. M., α-N-Heteroarylation and α-Azidation of Ketones via Enolonium Species. *J. Org. Chem.* **2018,** *83*, 2442-2447.
51. Frisch, M. J.; Trucks, G. W.; Schlegel, H. B.; Scuseria, G. E.; Robb, M. A.; Cheeseman, J. R.; Scalmani, G.; Barone, V.; Petersson, G. A.; Nakatsuji, H., et al. *Gaussian 16 Rev. C.01*, Wallingford, CT, 2016.
52. Fuentealba, P.; Preuss, H.; Stoll, H.; Von Szentpály, L., A proper account of core-polarization with pseudopotentials: single valence-electron alkali compounds. *Chem. Phys. Lett.* **1982,** *89*, 418-422.
53. Rassolov, V. A.; Ratner, M. A.; Pople, J. A.; Redfern, P. C.; Curtiss, L. A., 6-31G* basis set for third-row atoms. *J. Comput. Chem.* **2001,** *22*, 976-984.

54. Weigend, F.; Ahlrichs, R., Balanced basis sets of split valence, triple zeta valence and quadruple zeta valence quality for H to Rn: Design and assessment of accuracy. *Phys. Chem. Chem. Phys.* **2005,** *7*, 3297-3305.
55. Barone, V.; Cossi, M., Quantum calculation of molecular energies and energy gradients in solution by a conductor solvent model. *J. Phys. Chem. A* **1998,** *102*, 1995-2001.
56. Ho, J., Are thermodynamic cycles necessary for continuum solvent calculation of pKas and reduction potentials? *Phys. Chem. Chem. Phys.* **2015,** *17*, 2859-2868.
57. Ribeiro, R. F.; Marenich, A. V.; Cramer, C. J.; Truhlar, D. G., Use of Solution-Phase Vibrational Frequencies in Continuum Models for the Free Energy of Solvation. *J. Phys. Chem. B* **2011,** *115*, 14556-14562.
58. Marcus, R. A., On the theory of oxidation-reduction reactions involving electron transfer. I. *J. Chem. Phys.* **1956,** *24*, 966-978.
59. Saveant, J. M., A simple model for the kinetics of dissociative electron transfer in polar solvents. Application to the homogeneous and heterogeneous reduction of alkyl halides. *J. Am. Chem. Soc.* **1987,** *109*, 6788-6795.

TOC graphic

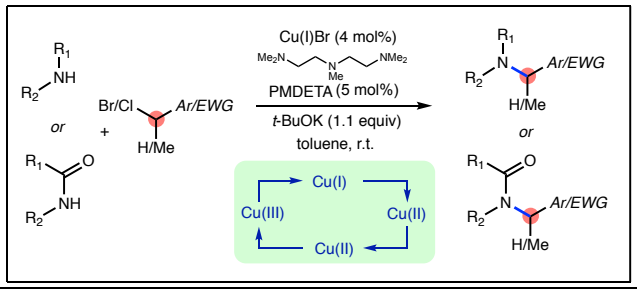
Cu(I)Br (4 mol%)
PMDETA (5 mol%)
t-BuOK (1.1 equiv)
toluene, r.t.
or
or
Br/Cl
Ar/EWG
H/Me
Cu(I)
Cu(II)
Cu(II)
Cu(III)